

## Cost of inferred nuclear parameters towards the f-mode dynamical tide in binary neutron stars

BIKRAM KESHARI PRADHAN ,<sup>1</sup> TATHAGATA GHOSH ,<sup>1</sup> DHRUV PATHAK ,<sup>1</sup> AND DEBARATI CHATTERJEE <sup>1</sup>

<sup>1</sup>*Inter University Centre for Astronomy and Astrophysics, Pune, Maharashtra, 411007, India*

### ABSTRACT

Gravitational Wave (GW) observations from Neutron Stars (NS) in a binary system provide an excellent scenario to constrain the nuclear parameters. The investigation of Pratten et al. (2022) has shown that the ignorance of f-mode dynamical tidal correction in the GW waveform model of the binary neutron star (BNS) system can lead to substantial bias in the measurement of NS properties and NS equations of state (EOS). In this work, we investigate the bias in the nuclear parameters resulting from the ignorance of dynamical tidal correction. In addition, this work demonstrates the sensitivity of the nuclear parameters and the estimated constraints on nuclear parameters and NS properties from future GW observations. We infer the nuclear parameters from GW observations by describing the NS matter within the relativistic mean field model. For a population of GW events, we notice that the ignorance of dynamical tide predicts a lower median for nucleon effective mass ( $m^*$ ) by  $\sim 6\%$  compared to the scenario when dynamical tidal correction is considered. Whereas at a 90% credible interval(CI),  $m^*$  gets constrained up to  $\sim 5\%$  and  $\sim 3\%$  in A+ (the LIGO-Virgo detectors with a sensitivity of 5th observing run) and Cosmic Explorer (CE) respectively. We also discuss the resulting constraints on all other nuclear parameters, including compressibility, symmetry energy, and slope of symmetry energy, considering an ensemble of GW events. We do not notice any significant impact in analyzing nuclear parameters other than  $m^*$  due to the ignorance of f-mode dynamical tides.

### 1. INTRODUCTION

Neutron stars (NS) provide a natural laboratory to explore the ultra-high dense matter under extreme conditions, such as high magnetic field and rotation, that are beyond the reach of the terrestrial experiments (Lattimer 2021). The NS macroscopic properties relate to the microscopic description of the NS matter via the pressure density relationship, more commonly known as the equation of state (EOS). The measurement of NS observables such as mass ( $M$ ) and radius ( $R$ ) with electromagnetic observations (Riley et al. 2021; Miller et al. 2021) at multiple wavelengths have significantly improved our understanding regarding the NS interior and the NS EOS. Additionally, the binary neutron star (BNS) mergers are sources of gravitational waves (GW). In a BNS merger, the tidal deformation of the NSs depends upon the NS interior, and hence, the measurement of the tidal deformability parameter is used to constrain the NS EOS in combination with mass measurements from the same binary. The detection of BNS events GW170817 (Abbott et al. 2017a, 2018, 2017b, 2019a,b) and GW190425 (Abbott et al. 2020a, 2021) by the LIGO-Virgo collaboration (Aasi et al. 2015; Acernese et al. 2015) have been widely used to understand the NS interior (Most et al. 2018; Biswas et al. 2021;

Bauswein et al. 2017; Essick et al. 2021; Huth et al. 2022; Annala et al. 2018; Fattoyev et al. 2018) and have opened a new window in the multimessenger astronomy.

The tidal deformation of the stars in a BNS contributes to the phase of the GW signal. The dominant contribution arises from the electric type quadrupolar adiabatic tidal deformation appearing first at 5 post-Newtonian (PN) order (Hinderer et al. 2010), and this has been used to infer the NS properties from the detected BNS candidates. A significant amount of effort has been made to develop an accurate waveform model, including different corrections such as the inclusion of higher order electric and magnetic multipolar tidal corrections (Hinderer et al. 2010; Bini et al. 2012; Damour & Nagar 2010; Landry & Poisson 2015; Banijahshemi & Vines 2020; Poisson 2020; Henry et al. 2020; Mandal et al. 2023) and the dynamical tidal correction due to resonant/non-resonant excitation of NS oscillation modes (Hinderer et al. 2016; Steinhoff et al. 2016; Schmidt & Hinderer 2019; Kuan & Kokkotas 2022; Pnigouras et al. 2022; Gamba & Bernuzzi 2022; Gupta et al. 2021; Gupta et al. 2023; Mandal et al. 2023; Abac et al. 2023). Although, for the detected events GW170817 and/or GW190425, there is a minor impact on the inferred NS properties due to the additional corrections of multipolar tidal effects (Godzieba et al. 2021; Pradhan et al. 2023c; Narikawa 2023) or due to the consideration of the dynamical corrections (Pratten et al.

2020; Gamba & Bernuzzi 2022; Pradhan et al. 2023c; Abac et al. 2023), their importance will be significant for future events accessible with increasing sensitivity of the current GW detectors or even with the next generation detectors. Furthermore, GW models, including dynamical tides, show better agreement with the numerical relativity simulations (Hinderer et al. 2016; Steinhoff et al. 2016; Andersson & Pnigouras 2019; Schmidt & Hinderer 2019). The recent investigation of Pratten et al. (2022) suggests that the ignorance of f-mode dynamical tides can sufficiently bias the measurement of NS tidal deformability, leading to the biased inference of the EOS.

The simultaneous measurements of mass and tidal deformability of the NSs from GW measurements play a crucial role in improving the uncertainty in the nuclear physics (Güven et al. 2020; Ghosh et al. 2022; Ghosh et al. 2022a; Biswas et al. 2021; Lattimer 2021; Pradhan et al. 2023a; Mondal & Gulminelli 2023; Huang et al. 2023; Beznogov & Raduta 2023; Traversi et al. 2020; Pradhan et al. 2023b; Patra et al. 2022; Imam et al. 2022). As the ignorance of the f-mode dynamical tides substantially affects the measurement of NS EOS and NS properties, this leads us to question how much bias one would expect on the nuclear parameters constrained using GW observations due to ignorance of f-mode dynamical tides. In the context of NS physics, the EOS models based on the inclusion of interaction among the NS constituents are classified into two main subgroups: (i) microscopic or *ab-initio* (Oertel et al. 2017a; Sabatucci et al. 2022) and (ii) phenomenological models described by effective theories with parameters fitted to reproduce saturation nuclear parameters and/or nuclear properties (Machleidt et al. 1987). As our main concern is to study the bias in the nuclear parameters, we adopt the phenomenological relativistic mean field (RMF) model whose model parameters are calibrated to nuclear parameters (Hornick et al. 2018; Chen & Piekarewicz 2014a).

The recent study by Iacovelli et al. (2023) focuses on constraining nuclear parameters based on forthcoming GW observations. However, contrary to the meta-model approach used in Iacovelli et al. (2023), our work differs by using the RMF description of the NS EOS. The comprehensive investigation in the study by Iacovelli et al. (2023) employs the Fisher matrix analysis for GW parameter inference. However, a thorough comparison of the Fisher matrix analysis with the complete Bayesian analysis in Iacovelli et al. (2023) reveals that the Fisher matrix approach falls short in accurately estimating the errors associated with NS properties in certain cases. As our analysis involves posterior distributions of individual tidal parameters, we perform the Bayesian parameter estimation instead of the Fisher matrix analysis. Furthermore, the recent work from (Walker et al. 2024) discusses the recession constraints on the NS EOS with the next-generation gravitational wave detector us-

ing the spectral decomposition method (Lindblom 2010) to describe the NS EOS.

In this work, we try to translate the bias in the measured NS properties from GW events due to ignorance of f-mode dynamical tide in the nuclear parameters in a Bayesian formalism. The work is organized in the following way. In Sec. 2, we discuss the methodology of our work, including the choice of GW events, detector configurations, and Bayesian formalism. We discuss our results in Sec. 3 and conclude our findings in Sec. 4.

## 2. METHODOLOGY

To investigate the impact of f-mode dynamical tides, we model the GW with the frequency domain TaylorF2 waveform model including 3.5PN point particle phase, adiabatic tidal effects up to 7.5PN order accounting for the impact from magnetic deformation ( $\Sigma_2$ ), and the octupolar tidal deformability ( $\Lambda_3$ ) Henry et al. (2020): we represent this waveform as  $\text{TF2}_{\text{AT}}$ . Additionally, we include the ready-to-use quadrupolar f-mode dynamical tidal correction from Schmidt & Hinderer (2019) to TF2<sub>AT</sub> waveform model and represent this as TF2<sub>DT</sub>.

As discussed in Pratten et al. (2022), the impact of the dynamical tide is significant for the 5th observation run (O5) of LIGO-Virgo detectors (LIGO Scientific Collaboration et al. 2015; Acernese et al. 2015) and even for next-generation detectors. So, we focus on the GW events detected by LIGO-Virgo detectors with A+ sensitivity (as anticipated for the 5th observation run) (Abbott et al. 2020b; LVK 2022) and the next-generation detector, cosmic explorer (CE) (Evans et al. 2021; Reitze et al. 2019; Hall et al. 2021; Kuns et al. 2023). We consider uniform mass distribution between  $M_{\min} = 1 M_{\odot}$  and maximum mass  $M_{\max}$  for each component mass. The choice of  $M_{\min}$  is consistent with the predicted lower bound of NS mass from plausible supernova formation channels (Fryer et al. 2012; Woosley et al. 2020). The maximum mass is determined from the injected EOS. The other relevant properties, such as the tidal deformability parameters of electric type  $\Lambda_{\ell=\{2,3\}}$ , magnetic type  $\Sigma_2$ , and f-mode angular frequency  $\omega_2$  are assigned to the NSs assuming a particular nuclear parametrization<sup>1</sup> given in the injection column of table 1 with the EOS model described in Hornick et al. (2018). The sources are distributed isotropically over the sky and within the luminosity distance ( $d_L$ ) of 200 Mpc following Madau-Dickinson star formation rate (Madau & Dickinson 2014). We assume Planck15 cosmology (Planck Collaboration et al. 2016) in this entire work. For the injection and recovery studies discussed in Sec. 3.2, we ignore the spin of individual NSs.

<sup>1</sup> The particular parameterization is considered for the RMF model given in section 2.1 (for which we are aiming to constrain the nuclear parameters), and it also satisfies the state-of-the-art constraints such as Chiral Effective Field Theory and current astrophysical data.

Furthermore, considering a local merger rate of  $\sim 450 \text{ Gpc}^{-3} \text{ yr}^{-1}$  (Abbott et al. 2023), we expect  $\sim 13$  BNS events per year.

Next, we perform parameter estimation using the dynamic nested sampler `dynesty` Speagle (2020) as implemented in the parameter estimation package `bilby_pipe` (Ashton et al. 2019) for individual BNS events. We consider uniform prior over detector-frame component-masses ( $m_{1,2}^z = m_{1,2}(1+z)$ , where  $m_{1,2}$  are source-frame masses at redshift  $z$ ) and the corresponding tidal deformabilities ( $\Lambda_{1,2}$ ). We also assume a power law prior for luminosity distance ( $d_L^2$ ) and isotropic prior for inclination angle. For the additional parameters, such as  $\Lambda_3, \Sigma_2$ , and  $\omega_2$ , we use the universal relations from Pradhan et al. (2023c). The remaining BNS parameters (such as sky position) are kept fixed at their injected values to reduce the computational cost. However, one should ideally use broad enough priors for all the source parameters. This is a simplification in this work that should be improved in the future to investigate the uncertainties and systematics in inferred EoS parameters. The posteriors thus obtained will be utilized further to constrain the EOS parameters as follows:

$$p(\mathcal{E} | \{d\}) \propto \pi(\mathcal{E}) \prod_i \int \mathcal{L}(d_i | \theta_i) \pi_{\text{pop}}(\theta_i | \mathcal{E}) d\theta_i \quad (1)$$

where,  $\theta = \{m_1, m_2, d_L, \Lambda_1, \Lambda_2\}$  represent the source parameters of the individual source, denoted by the subscript  $i$ . Since we are only interested in inferring EOS parameters from  $m - \Lambda$  relation and fixing the population, the selection effect has not been included in Eq. (1). In Eq. (1), the semi-marginalized likelihood  $\mathcal{L}$  has been calculated by dividing the priors  $\pi_{\text{PE}}(\theta)$  from the corresponding posteriors  $p(\theta | d)$  while performing the parameter estimation for NS properties using `bilby_pipe`:

$$\mathcal{L}(d | \theta) \propto \frac{p(\theta | d)}{\pi_{\text{PE}}(\theta)} \quad (2)$$

We have implemented the Gaussian kernel density estimator from `Statsmodel` (Seabold & Perktold 2010) to estimate the likelihood  $\mathcal{L}$  from the posterior samples of source parameters. Finally, the EOS parameters have been estimated by using the nested sampler `Pymultinest` (Buchner et al. 2014), as shown in Eq. (1).

### 2.1. Equations of State: RMF Model

The pressure density relationship:  $p = p(\epsilon)$ , referred to as the EOS, plays a vital role in relating the microscopic behavior of NS matter and the properties of the NS. We describe the NS matter with the relativistic mean field (RMF) model, which is a phenomenological model where the model parameters are calibrated to the nuclear parameters saturation data. In RMF theory, the

Lagrangian density describes the interaction between baryons through the exchange of mesons: the scalar-isoscalar ( $\sigma$ ), vector-isoscalar ( $\omega$ ), vector-isovector ( $\rho$ ) mesons as given in Eq. (3).

$$\begin{aligned} \mathcal{L} = & \sum_N \bar{\psi}_N (i\gamma^\mu \partial_\mu - m + g_\sigma \sigma - g_{\omega B} \gamma_\mu \omega^\mu - \frac{g_\rho}{2} \gamma_\mu \vec{\tau} \vec{\rho}^\mu) \psi_N \\ & + \frac{1}{2} (\partial_\mu \sigma \partial^\mu \sigma - m_\sigma^2 \sigma^2) - \frac{1}{3} b m (g_\sigma \sigma)^3 + \frac{1}{4} c (g_\sigma \sigma)^4 \\ & + \frac{1}{2} m_\omega^2 \omega_\mu \omega^\mu - \frac{1}{4} \omega_{\mu\nu} \omega^{\mu\nu} \\ & - \frac{1}{4} (\vec{\rho}_{\mu\nu} \cdot \vec{\rho}^{\mu\nu} - 2m_\rho^2 \vec{\rho}_\mu \vec{\rho}^\mu) + \Lambda_\omega (g_\rho^2 \vec{\rho}_\mu \vec{\rho}^\mu) (g_\omega^2 \omega_\mu \omega^\mu) \end{aligned} \quad (3)$$

where  $\Psi_N$  is the Dirac field of the nucleons N,  $m$  is the vacuum nucleon mass, while  $\gamma^\mu$  and  $\vec{\tau}$  are the Dirac and Pauli matrices respectively.  $\sigma$ ,  $\omega$ ,  $\rho$  denote the meson fields, with isoscalar coupling constants  $g_\sigma$ ,  $g_\omega$ , isovector coupling  $g_\rho$  and mixed  $\omega - \rho$  coupling  $\Lambda_\omega$ .  $b$  and  $c$  represent the scalar meson self-interaction.

The isoscalar set of couplings  $g_\sigma$ ,  $g_\omega$ ,  $b$  and  $c$  are determined by fixing the saturation density  $n_0$ , the binding energy per nucleon  $E_{\text{sat}}$ , the incompressibility coefficient  $K$  and the effective nucleon mass  $m^* = m_N - g_\sigma \sigma$  at saturation,  $m_N$  being the mass of the nucleon at the saturation. On the other hand, isovector couplings  $g_\rho$  and  $\Lambda_\omega$  are determined as a function of the symmetry energy  $J$  and the slope of the symmetry energy at saturation  $L$ . Complete descriptions regarding obtaining the energy density and pressure in the mean-field limit can be found at Hornick et al. (2018). Hence, given a set of nuclear parameters,  $\mathcal{E} = \{n_0, E_{\text{sat}}, K, m^*, L, J\}$ , a unique EOS can be obtained following the methodology given in Hornick et al. (2018). We fix the low density EOS to that of SLy (Gulminelli & Raduta 2015) and stitch it to the core EOS at a density  $< 0.5n_0$ , making the EOS thermodynamically stable and also satisfying the causality condition (i.e., speed of sound  $\leq 1$ ).

## 3. RESULTS

### 3.1. GW170817

Several investigations have been conducted to determine the impact of the dynamical tidal correction for the event GW170817 (Pratten et al. 2020; Gamba & Bernuzzi 2022; Pradhan et al. 2023c). Even though there is no statistically significant support (based on the Bayes factor comparison) for the inclusion of dynamical tidal corrections over adiabatic tides for the GW170817, the bias on the recovered tidal parameters cannot be disregarded (Gamba & Bernuzzi 2022; Pradhan et al. 2023c). This can be explained by looking at the relatively low sensitivity of the GW detector in the region where the dynamical tidal correction appears significant ( $\geq 800$  Hz, (Williams et al. 2022)).

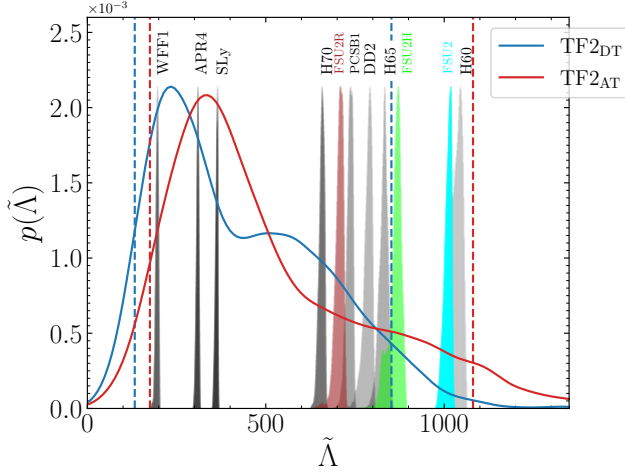


**Figure 1.** The probability distribution of  $\tilde{\Lambda}$  resulting from the BNS event GW170817 with (blue) and without (red) consideration of f-mode dynamical tidal correction. The 90% symmetric credible interval has also been shown with dashed lines. The distribution of  $\tilde{\Lambda}$  for a few EOS models has also been displayed. The probability distributions of  $\tilde{\Lambda}$  for representative EOS models are scaled to display them in one figure for better comparison.

We perform the Bayesian parameter estimation of GW170817 strain data (Rich Abbott & et al. 2021)<sup>2</sup> with the noise curve given in (Abbott et al. 2019b), using the dynamic nested sampler `dynesty` (Speagle 2020) as implemented in the parameter estimation package `bilby_pipe` (Ashton et al. 2019). In addition to the inspiral-only frequency domain TaylorF2 (TF2<sub>AT</sub> and TF2<sub>DT</sub>) waveform models described in Sec. 2, we also consider the spin orbit (Bohé et al. 2013) and spin-spin interaction corrections (Mishra et al. 2016) to the waveform model. Further details can be found in Pradhan et al. (2023c)<sup>3</sup>.

We show the posterior probability distribution of the reduced tidal deformability parameter  $\tilde{\Lambda}$  (see relation (5) from Wade et al. (2014) for the definition) resulting from waveform models TF2<sub>AT</sub> and TF2<sub>DT</sub> in fig. 1. Additionally, fig. 1 displays the distribution of  $\tilde{\Lambda}$  for a few representative EOSs: WFF1 (Wiringa et al. 1988), APR4 (Akmal et al. 1998), SLy4 (Chabanat et al. 1998; Gulminelli & Raduta 2015; Danielewicz & Lee 2009), PCSB1 (Pradhan et al. 2023a), DD2 (Typel et al. 2010) and the FSU2, FSU2H, FSU2R models from (Chen & Piekarewicz 2014b; Tolos et al. 2017; Negreiros et al. 2018; Grill et al. 2014). The aforementioned realistic EoSs are taken either from CompOSE database (Typel

et al. 2015; Oertel et al. 2017b; Typel et al. 2022) or from LALSimulation (LIGO Scientific Collaboration 2018). We have also shown the distributions of  $\tilde{\Lambda}$  corresponding to the Hornick parametrizations (Hornick et al. 2018) H60, H65, and H70, with different values for  $m^*/m_N = 0.6, 0.65$ , and  $0.70$ , respectively<sup>4</sup>. Though the distributions of  $\tilde{\Lambda}$  for RMF parametrized EoSs FSU2H, FSU2, H60 successfully fall within the 90% symmetric credible interval (CI) of  $\tilde{\Lambda}$  posterior recovered using TF<sub>AT</sub>, it does not fit within the 90% symmetric credible interval (CI) of  $\tilde{\Lambda}$  recovered using TF<sub>DT</sub>. This suggests that the nuclear parameters constrained using the GW detection can be affected by considering f-mode dynamical tidal corrections.

We perform the Bayesian analysis to constrain the EOS parameters described in Sec. 2. We consider uniform prior for each nuclear parameter  $x$  ranging from  $x_l$  to  $x_u$ , similar to the values given as the truncation limits in the prior column of table 1. For GW170817, considering a uniform prior in nuclear parameters, we find that only  $m^*$  and  $L$  get better constrained, but no noticeable constraint on the other nuclear parameters is observed. We compile the recovered distribution of  $m^*$  and  $L$  in fig. 4 of Appendix A. For GW170817, the consideration of TF2<sub>DT</sub> GW model does not impact the posterior of nuclear parameters that were recovered with TF2<sub>AT</sub> GW model. However, we notice a smaller value for the lower bound of  $m^*$  resulting in TF2<sub>DT</sub> GW model compared to what was recovered with TF2<sub>AT</sub>. This can be explained by looking at the higher upper limit of  $\tilde{\Lambda}$  with TF2<sub>AT</sub>, demanding stiffer EoSs and resulting in a smaller lower bound on  $m^*$ .

### 3.2. Injection Studies

The impact of f-mode dynamical tide becomes significant with the increasing sensitivity of the current detectors or even for the next generation detectors Pratten et al. (2022). We consider two different detector network configurations. The first one consists of two LIGO detectors ( LIGO-Hanford(H) and LIGO-Livingston (L)) with the A+ design sensitivity, as anticipated for the fifth observing run (O5) and the Virgo detector(V) operating at the low-limit sensitivity (LVK 2022) (similar to that of Pratten et al. (2022)). The other network consists of two Cosmic Explorer (CE) detectors (Evans et al. 2021; Reitze et al. 2019), located at Hanford and Livingston, operating at their designed sensitivity (Kuns et al. 2023). Since the simulated sources are at low redshifts, all the events have a significant network signal-to-noise ratio (SNR) of  $\geq 30$  and  $\geq 200$  for A+ and CE configuration, respectively.

To study the bias due to ignorance of f-mode dynamical tides, we obtain the posteriors of GW parameters

<sup>2</sup> <https://www.gw-openscience.org/events/GW170817/>

<sup>3</sup> We have not used the “relative binning” methodology here to find the posterior of the BNS event GW170817, as done in our previous work Pradhan et al. (2023c).

<sup>4</sup> The other nuclear parameters are fixed at  $n_0 = 0.15 \text{ fm}^{-3}$ ,  $E_{sat} = -16 \text{ MeV}$ ,  $K = 240 \text{ MeV}$ ,  $L = 60 \text{ MeV}$ ,  $J = 32 \text{ MeV}$

using both  $\text{TF2}_{\text{AT}}$  and  $\text{TF2}_{\text{DT}}$  waveform models individually while keeping the injection waveform to  $\text{TF2}_{\text{DT}}$ , i.e., the dynamical correction is always considered during the injection. We perform the parameter estimation for the GW parameters and the nuclear parameters for the simulated events described in Sec. 2. We employ a truncated Gaussian prior for each of the nuclear parameters ( $x$ ) with a mean ( $\mu_x$ ) fixed to the parameters of injected PCSB0 EOS model and the standard deviation ( $\sigma_x$ ) inspired from Margueron et al. (2018). We truncate each normal distribution for parameter  $x$  within the range, defined by the minimum value  $x_l$  and the maximum value  $x_u$ , i.e, the prior of  $x$  is taken as  $\pi(x) = \mathcal{N}(\mu_x, \sigma_x) T[x_l, x_u]$ .

We display the joint posteriors of the recovered nuclear parameters in fig. 2 and fig. 3 from 13 BNS events with A+ and CE configurations, respectively. We have tabulated the median and 90% symmetric CI of the EOS parameters recovered with both  $\text{TF2}_{\text{AT}}$  and  $\text{TF2}_{\text{DT}}$  waveform models in table 1. In addition to the nuclear parameters, we have also shown the distributions of radius ( $R_{1.4M_\odot}$ ) and tidal deformability ( $\Lambda_{1.4M_\odot}$ ) of a canonical  $1.4M_\odot$  NS star reconstructed from the nuclear parameters resulting from different network configurations and different GW waveform models in figs. 2 and 3. Although we perform the parameter estimation of nuclear parameters, we have shown the equivalent priors of  $R_{1.4M_\odot}$ , and  $\Lambda_{1.4M_\odot}$  in figs. 2 and 3 corresponding to the priors of the nuclear parameters. From fig. 2, one can conclude that with a set of BNS events detected in A+, the nuclear parameters get well-constrained, and especially the determination of nuclear parameters  $n_0$ ,  $L$ , and  $J$  improves significantly with consideration of BNS events with CE configuration. Additionally,  $m^*$  gets significantly constrained to 5% with A+, and the uncertainty is further reduced to 3% considering CE network configuration. A better constraint on  $m^*$  ( $\Delta m^*_{90\%} \leq 5\%$ ) is expected, as, in the considered RMF model,  $m^*$  controls the stiffness of the EOSs as well as shows strong correlations with NS observables (Hornick et al. 2018; Pradhan et al. 2023a; Ghosh et al. 2022; Pradhan et al. 2022).

Furthermore, one can find the overlapping region for most of the EOS parameters recovered with  $\text{TF2}_{\text{AT}}$  and  $\text{TF2}_{\text{DT}}$ . However, the distribution of  $m^*$  under two different waveform models seems to be distinct. The ignorance of dynamical tide estimates a lower  $m^*$  by  $\sim 6\%$  compared to the value of  $m^*$  obtained considering the dynamical tidal correction. The ignorance of dynamical tide estimates a higher  $\Lambda$  value (see, Pratten et al. (2022)) that requires a stiffer EOS. In contrast,  $\text{TF2}_{\text{DT}}$  provides the lower estimate for  $\Lambda$ , which can be explained with the softer EOSs. Hence, the ignorance of dynamical tide predicts a lower  $m^*$  compared to the value of  $m^*$  resulting from the inclusion of dynamical tides, such that the posterior produces sufficiently stiff EOSs to explain the higher  $\Lambda$  values. For completeness,

we have also displayed the bias on EOS and  $M - R$  relations recovered from the posteriors of nuclear parameters in Appendix B. The trend in  $M - R$  relation and the properties of  $1.4M_\odot$  due to ignorance of dynamical tide resulting with the considered RMF model seems to be in excellent agreement with the results from Pratten et al. (2022)<sup>5</sup>.

#### 4. DISCUSSIONS

We analyze the impact of the inclusion of f-mode dynamical tidal correction in the GW model on the nuclear parameters inferred from GW observations. For the BNS event GW170817, we do not find any substantial impact on the nuclear parameters due to consideration of dynamical tidal correction apart from a smaller lower bound on  $m^*$  due to the ignorance of dynamical tide. For future events, all nuclear parameters other than  $m^*$  are recovered well even after ignorance of f-mode dynamical tides. With consideration of an ensemble of BNS events in A+, the ignorance of f-mode dynamical corrections lowers the median of  $m^*$  ( $\sim 6\%$ ) compared to the median of  $m^*$  recovered with consideration of f-mode dynamical tide. In contrast, the value of  $m^*$  is constrained up to 5% (within 90% CI). Furthermore, with the simulated BNS events in the CE network configuration,  $m^*$  gets constrained up to  $\sim 3\%$  ( $\leq 90\%$  CI) with a bias of  $\sim 6\%$  on the median due to ignorance of dynamical tidal correction. We have also discussed how well the other nuclear parameters, such as  $n_0, E_{\text{sat}}, K, J$ , and  $L$  get constrained with an ensemble of BNS events in the framework of the RMF model. Any biases in these GW measurements can directly impact our understanding of nuclear physics. Therefore, having an accurate description of the GW waveform model is one of the key requirements. Notably, our work sheds light on the impact of dynamical tidal corrections on nuclear physics, especially when constrained by GW observations. This contribution holds significant importance in revealing these effects and advancing our understanding of the intricate interplay between GW astronomy and nuclear physics.

This work can be further improved by considering the additional corrections, such as spin and eccentricity, to the GW model considered in Sec. 3.2 for future events. It has been discussed that the consideration of spin and eccentricity further enhances the excitation of oscillation modes of NSs (Kuan & Kokkotas 2022; Steinhoff et al. 2021; Pnigouras et al. 2022) and may affect GW, and therefore need to be implemented. The EOS model for connecting the nuclear parameter and NS matter is specific to a nucleonic RMF model. Further studies can be performed by considering different NS matter compositions or with other EOS models connecting to nuclear and hypernuclear parameters.

<sup>5</sup> Polytropic EOS model is considered to describe the NS matter

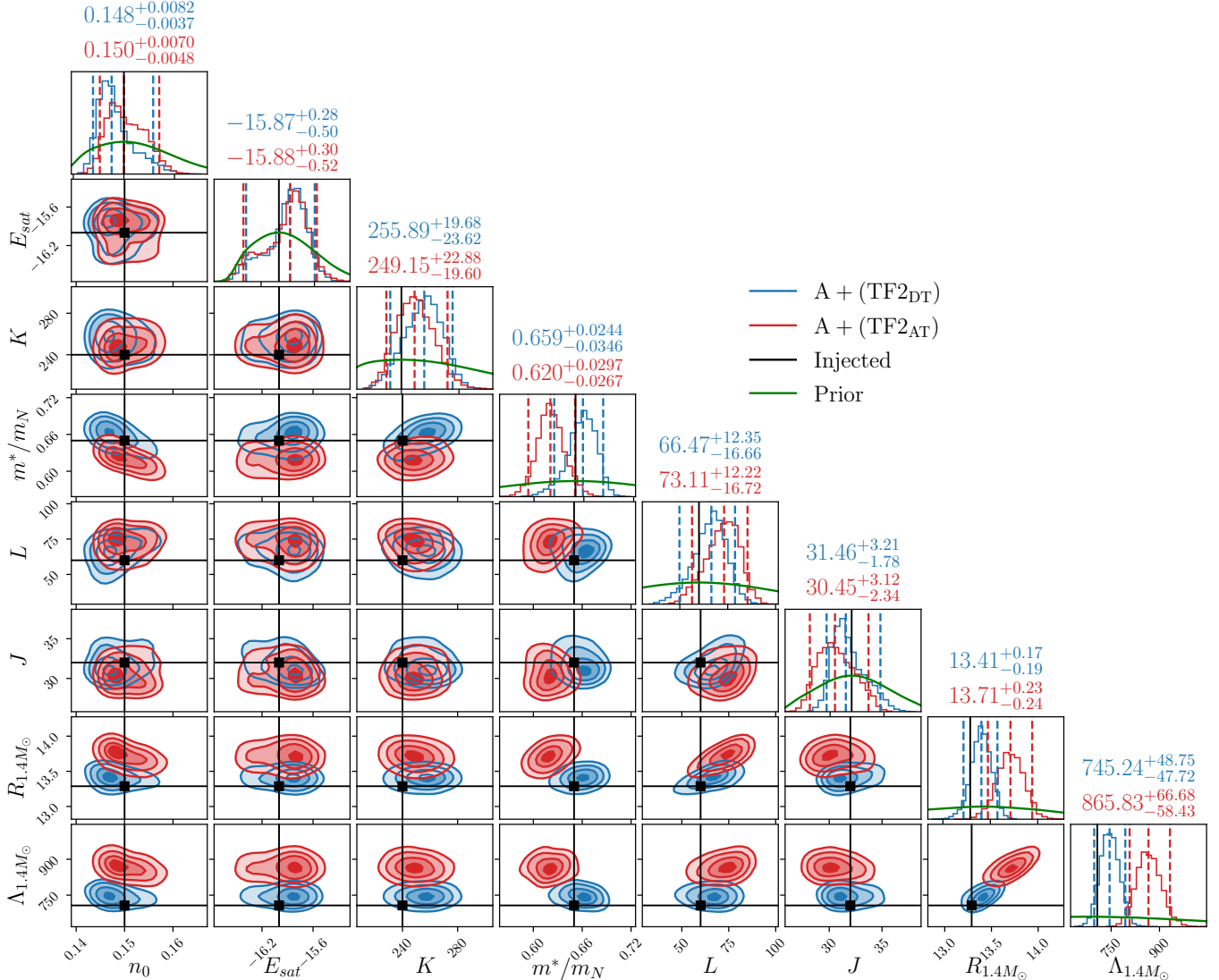


**Figure 2.** Joint and marginalized posterior distribution of nuclear parameters resulting from 13 BNS events in A+ configuration with (blue) and without (red) consideration of f-mode dynamical correction in the GW model during recovery of NS properties from simulated GW events, while injections are done with the inclusion of dynamical tidal correction. The median, the upper, and the lower bound correspond to the symmetric 90% credible interval are also mentioned. The injection values are shown with black lines, and the priors are displayed in green. The units of nuclear parameters are mentioned in table 1 and  $R_{1.4M_\odot}$  is in units of km.

In this work, we assume the mass distribution of BNS is precisely known, which is not the case in the real data. Furthermore, it is essential to infer NS EOS and mass distribution simultaneously to alleviate the biases arising from individual analyses (Wysocki et al. 2020; Golomb & Talbot 2022). The Bayesian formalism employed in this work can be further improved by incorporating the cosmological parameters Ghosh et al. (2022b). However, the most favorable approach would involve the joint fitting of astrophysical distribution as well as cosmological parameters for accurate inference of NS EOS (Ghosh et al. 2023). Additionally, it may be essential to incorporate the spin distribution of BNS as

well (Biscoveanu et al. 2022), which needs to be studied in the future. Further improvements in constraining the NS EOS can be achieved by incorporating joint information from existing electromagnetic (EM) observations and future observations, including those from space X-ray and  $\gamma$ -ray observatories, along with GW observations<sup>6</sup>.

<sup>6</sup> The constraints on the NS properties such as the moment of inertia and NS radius in light of future NS measurements with GW and X-ray observations has been addressed recently in (Suleiman & Read 2024).

Parameter	Injection	Prior	Posterior	
			A+ TF2 <sub>DT</sub> (TF2 <sub>AT</sub> )	CE-CE TF2 <sub>DT</sub> (TF2 <sub>AT</sub> )
$n_0 [\text{fm}^{-3}]$	0.15	$\mathcal{N}(0.15, 0.006) T[0.14, 0.18]$	$0.148_{-0.0037}^{+0.0082}$ ( $0.150_{-0.0048}^{+0.0070}$ )	$0.148_{-0.0020}^{+0.0023}$ ( $0.147_{-0.0017}^{+0.0022}$ )
$E_{\text{sat}} [\text{MeV}]$	-16.0	$\mathcal{N}(-16, 0.40) T[-16.5, -15]$	$-15.87_{-0.50}^{+0.28}$ ( $-15.88_{-0.52}^{+0.30}$ )	$-15.69_{-0.46}^{+0.24}$ ( $-15.71_{-0.34}^{+0.18}$ )
$K [\text{MeV}]$	240	$\mathcal{N}(240, 50) T[200, 355]$	$256_{-24}^{+20}$ ( $249_{-20}^{+23}$ )	$250_{-29}^{+20}$ ( $253_{-25}^{+15}$ )
$m^*/m_N$	0.65	$\mathcal{N}(0.65, 0.09) T[0.4, 0.9]$	$0.659_{-0.035}^{+0.024}$ ( $0.620_{-0.027}^{+0.03}$ )	$0.657_{-0.015}^{+0.014}$ ( $0.620_{-0.014}^{+0.011}$ )
$L [\text{MeV}]$	60	$\mathcal{N}(60, 35) T[1, 140]$	$66_{-17}^{+12}$ ( $73_{-17}^{+12}$ )	$58_{-6}^{+7}$ ( $62_{-6}^{+9}$ )
$J [\text{MeV}]$	32	$\mathcal{N}(32, 3) T[26, 39]$	$31.46_{-1.78}^{+3.21}$ ( $30.45_{-2.34}^{+3.12}$ )	$32_{-1.58}^{+1.65}$ ( $31.2_{-2.46}^{+1.81}$ )

**Table 1.** The median and 90% symmetric credible interval of the recovered posterior of nuclear parameters resulting from different scenarios considered in this work. The parameters of injected EOS are also tabulated in the injection column. The priors considered in the work are truncated Gaussian distributions with mean at the injected value and deviations are inspired from Margueron et al. (2018). We also truncate the distribution of nuclear parameters in a range that includes the minimum and maximum values, resulting from the phenomenological models as given in Margueron et al. (2018).

## 5. ACKNOWLEDGEMENTS

The authors are thankful to Geraint Pratten for carefully reviewing the manuscript and providing useful suggestions. B.K.P. would like to thank Aditya Vijaykumar for the helpful discussion on the GW waveform model and its implementation for GW parameter estimation. The authors gratefully acknowledge the use of the IUCAA LDG cluster Sarathi, accessed through the LIGO-Virgo-KAGRA Collaboration. B.K.P. is also grateful for the computational resource Pegasus, provided by IUCAA for the computing facility for the

computational/numerical work. This material is based upon work supported by NSF’s LIGO Laboratory, which is a major facility fully funded by the National Science Foundation. This work makes use of NumPy (van der Walt et al. 2011), SciPy (Virtanen et al. 2020), astropy (Astropy Collaboration et al. 2013, 2018, 2022), Matplotlib (Hunter 2007), jupyter (Kluyver et al. 2016), and pandas (Wes McKinney 2010) software packages. This document has been assigned to the LIGO document number LIGO-P2300407.

## APPENDIX

### A. DISTRIBUTION OF $M^*$ AND $L$ FOR GW170817

We display the joint and the marginalized distribution of  $m^*$  and  $L$  recovered for the BNS event GW170817 analyzed with the GW waveform model TF2<sub>AT</sub> and TF2<sub>DT</sub> in fig. 4. We do not notice any significant impact of the dynamical tidal correction on the nuclear parameters for the event GW170817.

### B. UNCERTAINTY IN EOS AND $M - R$ FROM FUTURE EVENTS

We reconstruct the NS EOS and the  $M - R$  posterior from the nuclear parameters recovered using 13 BNS events in A+ and displayed in figs. 5(a) and 5(b), re-

spectively. The substantial bias on the  $M - R$  recovered RMF model (shown in fig. 5(b)) due to ignorance of the f-mode dynamical tides is in agreement with the results of Pratten et al. (2020), where a polytropic description of NS matter is adopted. The uncertainty on the NS EOS and  $M - R$  relations resulting from the posterior of nuclear parameters recovered with BNS events in CE configuration is shown in figs. 6(a) and 6(b), respectively. As expected, with the increasing sensitivity of the CE detectors, the uncertainty on EOS or  $M - R$  decreases significantly compared to what is obtained with A+.

## REFERENCES

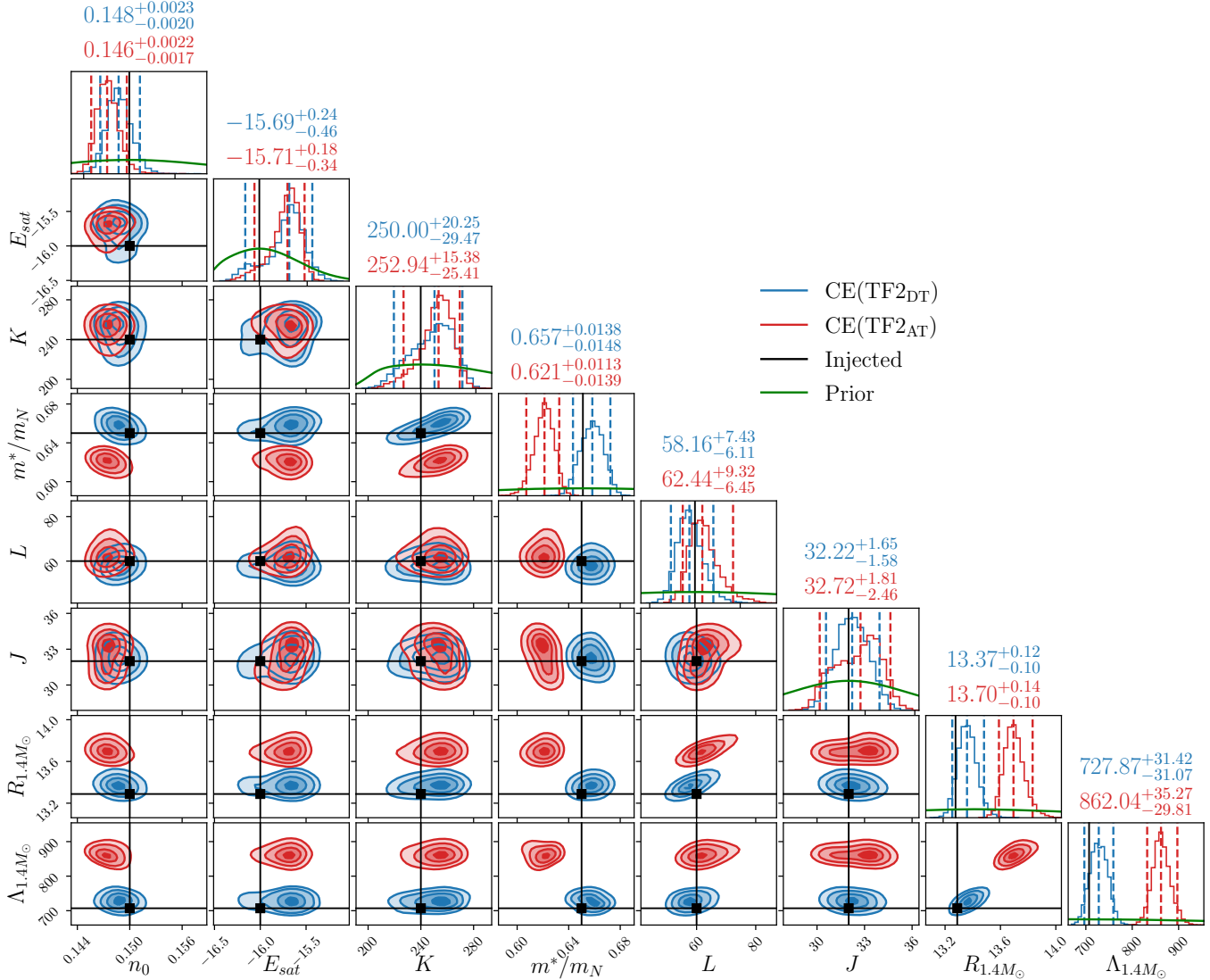


**Figure 3.** Same as fig. 2 but with CE detector configuration.

- Aasi, J., et al. 2015, *Class. Quant. Grav.*, 32, 074001,  
doi: [10.1088/0264-9381/32/7/074001](https://doi.org/10.1088/0264-9381/32/7/074001)
- Abac, A., Dietrich, T., Buonanno, A., Steinhoff, J., & Ujevic, M. 2023. <https://arxiv.org/abs/2311.07456>
- Abbott, B., Abbott, R., Abbott, T., et al. 2017a, *Physical Review Letters*, 119, doi: [10.1103/physrevlett.119.161101](https://doi.org/10.1103/physrevlett.119.161101)
- . 2017b, *The Astrophysical Journal*, 848, L12,  
doi: [10.3847/2041-8213/aa91c9](https://doi.org/10.3847/2041-8213/aa91c9)
- . 2018, *Physical Review Letters*, 121,  
doi: [10.1103/physrevlett.121.161101](https://doi.org/10.1103/physrevlett.121.161101)
- . 2019a, *Phys. Rev. X*, 9, 011001,  
doi: [10.1103/PhysRevX.9.011001](https://doi.org/10.1103/PhysRevX.9.011001)
- . 2019b, *Physical Review X*, 9, 031040,  
doi: [10.1103/PhysRevX.9.031040](https://doi.org/10.1103/PhysRevX.9.031040)

- . 2020a, *The Astrophysical Journal Letters*, 892, L3,  
doi: [10.3847/2041-8213/ab75f5](https://doi.org/10.3847/2041-8213/ab75f5)
- . 2021, *Physical Review X*, 11, 021053,  
doi: [10.1103/PhysRevX.11.021053](https://doi.org/10.1103/PhysRevX.11.021053)
- Abbott, B. P., Abbott, R., Abbott, T. D., et al. 2020b,  
*Living Reviews in Relativity*, 23, 3,  
doi: [10.1007/s41114-020-00026-9](https://doi.org/10.1007/s41114-020-00026-9)
- Abbott, R., Abbott, T. D., Acernese, F., et al. 2023,  
*Physical Review X*, 13, 011048,  
doi: [10.1103/PhysRevX.13.011048](https://doi.org/10.1103/PhysRevX.13.011048)
- Acernese, F., et al. 2015, *Class. Quant. Grav.*, 32, 024001,  
doi: [10.1088/0264-9381/32/2/024001](https://doi.org/10.1088/0264-9381/32/2/024001)
- Acernese, F., Agathos, M., Agatsuma, K., et al. 2015,  
*Classical and Quantum Gravity*, 32, 024001,  
doi: [10.1088/0264-9381/32/2/024001](https://doi.org/10.1088/0264-9381/32/2/024001)

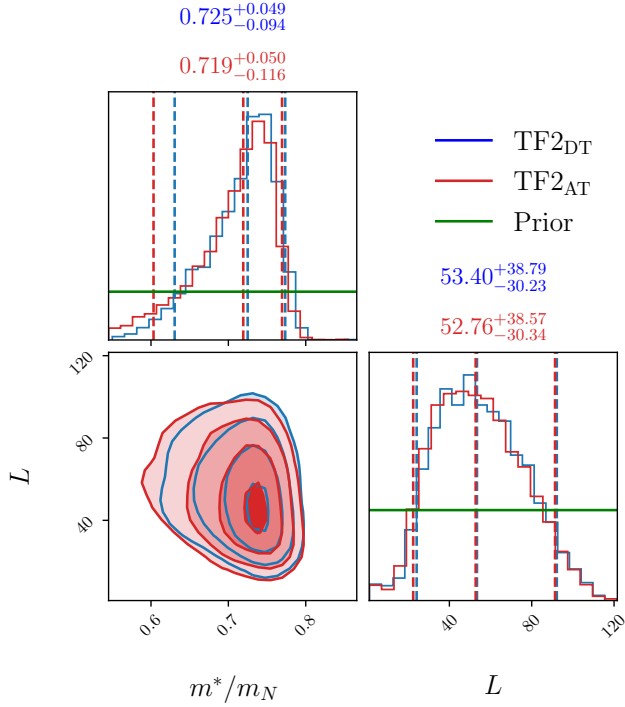


**Figure 4.** The joint and marginalized posterior distribution of  $m^*$  (in units of nucleon mass  $m_N$ ) and  $L$  (in MeV) resulting from the BNS event Gw170817 with (blue) and without (red) consideration of f-mode dynamical tidal correction in the GW model.

- Akmal, A., Pandharipande, V. R., & Ravenhall, D. G. 1998, Phys. Rev. C, 58, 1804, doi: [10.1103/PhysRevC.58.1804](https://doi.org/10.1103/PhysRevC.58.1804)
- Andersson, N., & Pnigouras, P. 2019, arXiv e-prints, arXiv:1905.00012, doi: [10.48550/arXiv.1905.00012](https://doi.org/10.48550/arXiv.1905.00012)
- Annala, E., Gorda, T., Kurkela, A., & Vuorinen, A. 2018, Phys. Rev. Lett., 120, 172703, doi: [10.1103/PhysRevLett.120.172703](https://doi.org/10.1103/PhysRevLett.120.172703)
- Ashton, G., Hübner, M., Lasky, P. D., et al. 2019, ApJS, 241, 27, doi: [10.3847/1538-4365/ab06fc](https://doi.org/10.3847/1538-4365/ab06fc)
- Astropy Collaboration, Robitaille, T. P., Tollerud, E. J., et al. 2013, A&A, 558, A33, doi: [10.1051/0004-6361/201322068](https://doi.org/10.1051/0004-6361/201322068)
- Astropy Collaboration, Price-Whelan, A. M., Sipőcz, B. M., et al. 2018, AJ, 156, 123, doi: [10.3847/1538-3881/aabc4f](https://doi.org/10.3847/1538-3881/aabc4f)
- Astropy Collaboration, Price-Whelan, A. M., Lim, P. L., et al. 2022, ApJ, 935, 167, doi: [10.3847/1538-4357/ac7c74](https://doi.org/10.3847/1538-4357/ac7c74)
- Banihashemi, B., & Vines, J. 2020, Phys. Rev. D, 101, 064003, doi: [10.1103/PhysRevD.101.064003](https://doi.org/10.1103/PhysRevD.101.064003)
- Bauswein, A., Just, O., Janka, H.-T., & Stergioulas, N. 2017, The Astrophysical Journal Letters, 850, L34, doi: [10.3847/2041-8213/aa9994](https://doi.org/10.3847/2041-8213/aa9994)
- Beznogov, M. V., & Raduta, A. R. 2023, Phys. Rev. C, 107, 045803, doi: [10.1103/PhysRevC.107.045803](https://doi.org/10.1103/PhysRevC.107.045803)

- Bini, D., Damour, T., & Faye, G. 2012, Phys. Rev. D, 85, 124034, doi: [10.1103/PhysRevD.85.124034](https://doi.org/10.1103/PhysRevD.85.124034)
- Biscoveanu, S., Talbot, C., & Vitale, S. 2022, Mon. Not. Roy. Astron. Soc., 511, 4350, doi: [10.1093/mnras/stac347](https://doi.org/10.1093/mnras/stac347)
- Biswas, B., Char, P., Nandi, R., & Bose, S. 2021, Phys. Rev. D, 103, 103015, doi: [10.1103/PhysRevD.103.103015](https://doi.org/10.1103/PhysRevD.103.103015)
- Bohé, A., Marsat, S., & Blanchet, L. 2013, Classical and Quantum Gravity, 30, 135009, doi: [10.1088/0264-9381/30/13/135009](https://doi.org/10.1088/0264-9381/30/13/135009)
- Buchner, J., Georgakakis, A., Nandra, K., et al. 2014, A&A, 564, A125, doi: [10.1051/0004-6361/201322971](https://doi.org/10.1051/0004-6361/201322971)
- Chabanat, E., Bonche, P., Haensel, P., Meyer, J., & Schaeffer, R. 1998, Nuclear Physics A, 635, 231, doi: [https://doi.org/10.1016/S0375-9474\(98\)00180-8](https://doi.org/10.1016/S0375-9474(98)00180-8)
- Chen, W.-C., & Piekarewicz, J. 2014a, Phys. Rev. C, 90, 044305, doi: [10.1103/PhysRevC.90.044305](https://doi.org/10.1103/PhysRevC.90.044305)
- . 2014b, Phys. Rev. C, 90, 044305, doi: [10.1103/PhysRevC.90.044305](https://doi.org/10.1103/PhysRevC.90.044305)
- Damour, T., & Nagar, A. 2010, Phys. Rev. D, 81, 084016, doi: [10.1103/PhysRevD.81.084016](https://doi.org/10.1103/PhysRevD.81.084016)
- Danielewicz, P., & Lee, J. 2009, Nuclear Physics A, 818, 36, doi: <https://doi.org/10.1016/j.nuclphysa.2008.11.007>
- Essick, R., Landry, P., Schwenk, A., & Tews, I. 2021, Phys. Rev. C, 104, 065804, doi: [10.1103/PhysRevC.104.065804](https://doi.org/10.1103/PhysRevC.104.065804)
- Evans, M., Adhikari, R. X., Afle, C., et al. 2021, arXiv e-prints, arXiv:2109.09882, doi: [10.48550/arXiv.2109.09882](https://doi.org/10.48550/arXiv.2109.09882)
- Fattoyev, F. J., Piekarewicz, J., & Horowitz, C. J. 2018, Phys. Rev. Lett., 120, 172702, doi: [10.1103/PhysRevLett.120.172702](https://doi.org/10.1103/PhysRevLett.120.172702)
- Fryer, C. L., Belczynski, K., Wiktorowicz, G., et al. 2012, ApJ, 749, 91, doi: [10.1088/0004-637X/749/1/91](https://doi.org/10.1088/0004-637X/749/1/91)
- Gamba, R., & Bernuzzi, S. 2022, arXiv e-prints, arXiv:2207.13106. <https://arxiv.org/abs/2207.13106>
- Ghosh, S., Chatterjee, D., & Schaffner-Bielich, J. 2022, European Physical Journal A, 58, 37, doi: [10.1140/epja/s10050-022-00679-w](https://doi.org/10.1140/epja/s10050-022-00679-w)
- Ghosh, S., Pradhan, B. K., Chatterjee, D., & Schaffner-Bielich, J. 2022a, Front. Astron. Space Sci., 9, 864294, doi: [10.3389/fspas.2022.864294](https://doi.org/10.3389/fspas.2022.864294)
- Ghosh, T., Biswas, B., & Bose, S. 2022b, Phys. Rev. D, 106, 123529, doi: [10.1103/PhysRevD.106.123529](https://doi.org/10.1103/PhysRevD.106.123529)
- Ghosh, T., et al. 2023, (in preparation)
- Godzieba, D. A., Gamba, R., Radice, D., & Bernuzzi, S. 2021, Phys. Rev. D, 103, 063036, doi: [10.1103/PhysRevD.103.063036](https://doi.org/10.1103/PhysRevD.103.063036)
- Golomb, J., & Talbot, C. 2022, Astrophys. J., 926, 79, doi: [10.3847/1538-4357/ac43bc](https://doi.org/10.3847/1538-4357/ac43bc)

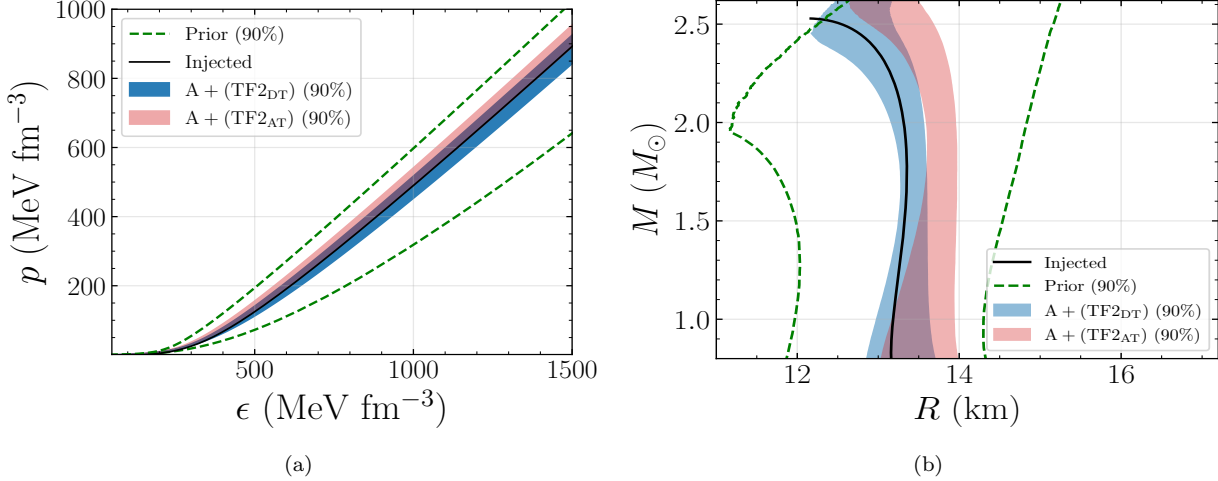


**Figure 5.** (a) 90% CI for pressure as a function of energy density and (b) 90% CI for radius as a function of mass reconstructed using the recovered nuclear parameters from the detection of 13 events in A+ network configuration, with (blue) and without (red) consideration of dynamical tidal correction in the recover GW model.

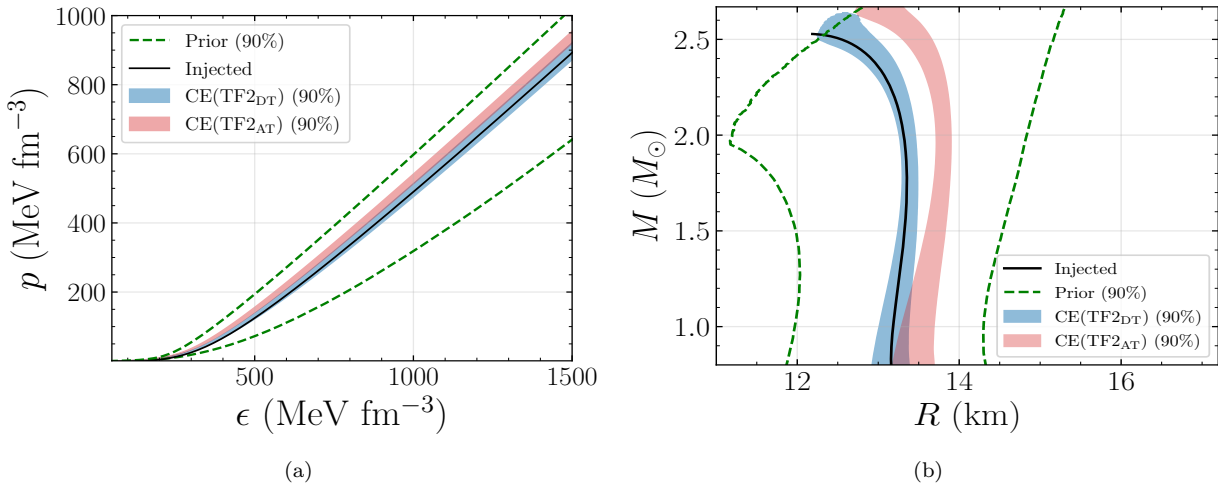


**Figure 6.** Same as fig. 5 but with CE detector network configuration.

- Grill, F., Pais, H., Providência, C. m. c., Vidaña, I., & Avancini, S. S. 2014, Phys. Rev. C, 90, 045803, doi: [10.1103/PhysRevC.90.045803](https://doi.org/10.1103/PhysRevC.90.045803)
- Gulminelli, F., & Raduta, A. R. 2015, Phys. Rev. C, 92, 055803, doi: [10.1103/PhysRevC.92.055803](https://doi.org/10.1103/PhysRevC.92.055803)
- Gupta, P. K., Steinhoff, J., & Hinderer, T. 2021, Phys. Rev. Res., 3, 013147, doi: [10.1103/PhysRevResearch.3.013147](https://doi.org/10.1103/PhysRevResearch.3.013147)
- Gupta, P. K., Steinhoff, J., & Hinderer, T. 2023, arXiv e-prints, arXiv:2302.11274, doi: [10.48550/arXiv.2302.11274](https://doi.org/10.48550/arXiv.2302.11274)
- Güven, H., Bozkurt, K., Khan, E., & Margueron, J. 2020, Phys. Rev. C, 102, 015805, doi: [10.1103/PhysRevC.102.015805](https://doi.org/10.1103/PhysRevC.102.015805)

- Hall, E. D., et al. 2021, Phys. Rev. D, 103, 122004, doi: [10.1103/PhysRevD.103.122004](https://doi.org/10.1103/PhysRevD.103.122004)
- Henry, Q., Faye, G., & Blanchet, L. 2020, Phys. Rev. D, 102, 044033, doi: [10.1103/PhysRevD.102.044033](https://doi.org/10.1103/PhysRevD.102.044033)
- Hinderer, T., Lackey, B. D., Lang, R. N., & Read, J. S. 2010, Phys. Rev. D, 81, 123016, doi: [10.1103/PhysRevD.81.123016](https://doi.org/10.1103/PhysRevD.81.123016)
- Hinderer, T., Taracchini, A., Foucart, F., et al. 2016, Phys. Rev. Lett., 116, 181101, doi: [10.1103/PhysRevLett.116.181101](https://doi.org/10.1103/PhysRevLett.116.181101)
- Hornick, N., Tolos, L., Zacchi, A., Christian, J.-E., & Schaffner-Bielich, J. 2018, Phys. Rev. C, 98, 065804, doi: [10.1103/PhysRevC.98.065804](https://doi.org/10.1103/PhysRevC.98.065804)

- Huang, C., Raaijmakers, G., Watts, A. L., Tolos, L., & Providência, C. 2023, arXiv e-prints, arXiv:2303.17518, doi: [10.48550/arXiv.2303.17518](https://doi.org/10.48550/arXiv.2303.17518)
- Hunter, J. D. 2007, Computing in Science & Engineering, 9, 90, doi: [10.1109/MCSE.2007.55](https://doi.org/10.1109/MCSE.2007.55)
- Huth, S., Pang, P. T. H., Tews, I., et al. 2022, Nature, 606, 276, doi: [10.1038/s41586-022-04750-w](https://doi.org/10.1038/s41586-022-04750-w)
- Iacobelli, F., Mancarella, M., Mondal, C., et al. 2023. <https://arxiv.org/abs/2308.12378>
- Imam, S. M. A., Patra, N. K., Mondal, C., Malik, T., & Agrawal, B. K. 2022, Phys. Rev. C, 105, 015806, doi: [10.1103/PhysRevC.105.015806](https://doi.org/10.1103/PhysRevC.105.015806)
- Kluyver, T., Ragan-Kelley, B., & et al. 2016, in Positioning and Power in Academic Publishing: Players, Agents and Agendas, ed. F. Loizides & B. Schmidt (Netherlands: IOS Press), 87–90. <https://eprints.soton.ac.uk/403913/>
- Kuan, H.-J., & Kokkotas, K. D. 2022, Phys. Rev. D, 106, 064052, doi: [10.1103/PhysRevD.106.064052](https://doi.org/10.1103/PhysRevD.106.064052)
- Kuns, K., Hall, E., Srivastava, V., et al. 2023, Cosmic Explorer Strain Sensitivity. <https://dcc.cosmicexplorer.org/CE-T2000017/public>
- Landry, P., & Poisson, E. 2015, Phys. Rev. D, 91, 104026, doi: [10.1103/PhysRevD.91.104026](https://doi.org/10.1103/PhysRevD.91.104026)
- Lattimer, J. 2021, Annual Review of Nuclear and Particle Science, 71, 433, doi: [10.1146/annurev-nucl-102419-124827](https://doi.org/10.1146/annurev-nucl-102419-124827)
- LIGO Scientific Collaboration. 2018, LIGO Algorithm Library - LALSuite, free software (GPL), doi: [10.7935/GT1W-FZ16](https://doi.org/10.7935/GT1W-FZ16)
- LIGO Scientific Collaboration, Aasi, J., Abbott, B. P., et al. 2015, Classical and Quantum Gravity, 32, 074001, doi: [10.1088/0264-9381/32/7/074001](https://doi.org/10.1088/0264-9381/32/7/074001)
- Lindblom, L. 2010, Phys. Rev. D, 82, 103011, doi: [10.1103/PhysRevD.82.103011](https://doi.org/10.1103/PhysRevD.82.103011)
- LVK. 2022, Noise curves used for Simulations in the update of the Observing Scenarios Paper. <https://dcc.ligo.org/LIGO-T2000012/public>
- Machleidt, R., Holinde, K., & Elster, C. 1987, Physics Reports, 149, 1, doi: [https://doi.org/10.1016/S0370-1573\(87\)80002-9](https://doi.org/10.1016/S0370-1573(87)80002-9)
- Madau, P., & Dickinson, M. 2014, ARA&A, 52, 415, doi: [10.1146/annurev-astro-081811-125615](https://doi.org/10.1146/annurev-astro-081811-125615)
- Mandal, M. K., Mastrolia, P., Silva, H. O., Patil, R., & Steinhoff, J. 2023. <https://arxiv.org/abs/2308.01865>
- Mandal, M. K., Mastrolia, P., Silva, H. O., Patil, R., & Steinhoff, J. 2023, arXiv e-prints, arXiv:2304.02030, doi: [10.48550/arXiv.2304.02030](https://doi.org/10.48550/arXiv.2304.02030)
- Margueron, J., Hoffmann Casali, R., & Gulminelli, F. 2018, Phys. Rev. C, 97, 025805, doi: [10.1103/PhysRevC.97.025805](https://doi.org/10.1103/PhysRevC.97.025805)
- Miller, M. C., Lamb, F. K., Dittmann, A. J., et al. 2021, The Astrophysical Journal Letters, 918, L28, doi: [10.3847/2041-8213/ac089b](https://doi.org/10.3847/2041-8213/ac089b)
- Mishra, C. K., Kela, A., Arun, K. G., & Faye, G. 2016, Phys. Rev. D, 93, 084054, doi: [10.1103/PhysRevD.93.084054](https://doi.org/10.1103/PhysRevD.93.084054)
- Mondal, C., & Gulminelli, F. 2023, Phys. Rev. C, 107, 015801, doi: [10.1103/PhysRevC.107.015801](https://doi.org/10.1103/PhysRevC.107.015801)
- Most, E. R., Weih, L. R., Rezzolla, L., & Schaffner-Bielich, J. 2018, Phys. Rev. Lett., 120, 261103, doi: [10.1103/PhysRevLett.120.261103](https://doi.org/10.1103/PhysRevLett.120.261103)
- Narikawa, T. 2023, arXiv e-prints, arXiv:2307.02033, doi: [10.48550/arXiv.2307.02033](https://doi.org/10.48550/arXiv.2307.02033)
- Negreiros, R., Tolos, L., Centelles, M., Ramos, A., & Dexheimer, V. 2018, The Astrophysical Journal, 863, 104, doi: [10.3847/1538-4357/aad049](https://doi.org/10.3847/1538-4357/aad049)
- Oertel, M., Hempel, M., Klähn, T., & Typel, S. 2017a, Rev. Mod. Phys., 89, 015007, doi: [10.1103/RevModPhys.89.015007](https://doi.org/10.1103/RevModPhys.89.015007)
- . 2017b, Rev. Mod. Phys., 89, 015007, doi: [10.1103/RevModPhys.89.015007](https://doi.org/10.1103/RevModPhys.89.015007)
- Patra, N. K., Sharma, B. K., Reghunath, A., Das, A. K. H., & Jha, T. K. 2022, Phys. Rev. C, 106, 055806, doi: [10.1103/PhysRevC.106.055806](https://doi.org/10.1103/PhysRevC.106.055806)
- Planck Collaboration, Ade, P. A. R., Aghanim, N., et al. 2016, A&A, 594, A13, doi: [10.1051/0004-6361/201525830](https://doi.org/10.1051/0004-6361/201525830)
- Pnigouras, P., Gittins, F., Nanda, A., Andersson, N., & Jones, D. I. 2022, arXiv e-prints, arXiv:2205.07577, doi: [10.48550/arXiv.2205.07577](https://doi.org/10.48550/arXiv.2205.07577)
- Poisson, E. 2020, Phys. Rev. D, 101, 104028, doi: [10.1103/PhysRevD.101.104028](https://doi.org/10.1103/PhysRevD.101.104028)
- Pradhan, B. K., Chatterjee, D., Gandhi, R., & Schaffner-Bielich, J. 2023a, Nuclear Physics A, 1030, 122578, doi: <https://doi.org/10.1016/j.nuclphysa.2022.122578>
- Pradhan, B. K., Chatterjee, D., Lanoye, M., & Jaikumar, P. 2022, Phys. Rev. C, 106, 015805, doi: [10.1103/PhysRevC.106.015805](https://doi.org/10.1103/PhysRevC.106.015805)
- Pradhan, B. K., Pathak, D., & Chatterjee, D. 2023b, Astrophys. J., 956, 38, doi: [10.3847/1538-4357/acef1f](https://doi.org/10.3847/1538-4357/acef1f)
- Pradhan, B. K., Vijaykumar, A., & Chatterjee, D. 2023c, Phys. Rev. D, 107, 023010, doi: [10.1103/PhysRevD.107.023010](https://doi.org/10.1103/PhysRevD.107.023010)
- Pratten, G., Schmidt, P., & Hinderer, T. 2020, Nature Commun., 11, 2553, doi: [10.1038/s41467-020-15984-5](https://doi.org/10.1038/s41467-020-15984-5)
- Pratten, G., Schmidt, P., & Williams, N. 2022, Phys. Rev. Lett., 129, 081102, doi: [10.1103/PhysRevLett.129.081102](https://doi.org/10.1103/PhysRevLett.129.081102)
- Reitze, D., Adhikari, R. X., Ballmer, S., et al. 2019, in Bulletin of the American Astronomical Society, Vol. 51, 35, doi: [10.48550/arXiv.1907.04833](https://doi.org/10.48550/arXiv.1907.04833)

- Rich Abbott, & et al. 2021, SoftwareX, 13, 100658, doi: <https://doi.org/10.1016/j.softx.2021.100658>
- Riley, T. E., Watts, A. L., Ray, P. S., et al. 2021, The Astrophysical Journal Letters, 918, L27, doi: [10.3847/2041-8213/ac0a81](https://doi.org/10.3847/2041-8213/ac0a81)
- Sabatucci, A., Benhar, O., Maselli, A., & Pacilio, C. 2022, arXiv e-prints, arXiv:2206.11286. <https://arxiv.org/abs/2206.11286>
- Schmidt, P., & Hinderer, T. 2019, Phys. Rev. D, 100, 021501(R), doi: [10.1103/PhysRevD.100.021501](https://doi.org/10.1103/PhysRevD.100.021501)
- Seabold, S., & Perktold, J. 2010, in Proceedings of the 9th Python in Science Conference, 92 – 96, doi: [10.25080/Majora-92bf1922-011](https://doi.org/10.25080/Majora-92bf1922-011)
- Speagle, J. S. 2020, Monthly Notices of the Royal Astronomical Society, 493, 3132, doi: [10.1093/mnras/staa278](https://doi.org/10.1093/mnras/staa278)
- Steinhoff, J., Hinderer, T., Buonanno, A., & Taracchini, A. 2016, Phys. Rev. D, 94, 104028, doi: [10.1103/PhysRevD.94.104028](https://doi.org/10.1103/PhysRevD.94.104028)
- Steinhoff, J., Hinderer, T., Dietrich, T., & Foucart, F. 2021, Phys. Rev. Res., 3, 033129, doi: [10.1103/PhysRevResearch.3.033129](https://doi.org/10.1103/PhysRevResearch.3.033129)
- Suleiman, L., & Read, J. 2024, arXiv e-prints, arXiv:2402.01948, doi: [10.48550/arXiv.2402.01948](https://doi.org/10.48550/arXiv.2402.01948)
- Tolos, L., Centelles, M., & Ramos, A. 2017, PASA, 34, e065, doi: [10.1017/pasa.2017.60](https://doi.org/10.1017/pasa.2017.60)
- Traversi, S., Char, P., & Pagliara, G. 2020, ApJ, 897, 165, doi: [10.3847/1538-4357/ab99c1](https://doi.org/10.3847/1538-4357/ab99c1)
- Typep, S., Oertel, M., & Klähn, T. 2015, Phys. Part. Nucl., 46, 633, doi: [10.1134/S1063779615040061](https://doi.org/10.1134/S1063779615040061)
- Typep, S., Röpke, G., Klähn, T., Blaschke, D., & Wolter, H. H. 2010, Phys. Rev. C, 81, 015803, doi: [10.1103/PhysRevC.81.015803](https://doi.org/10.1103/PhysRevC.81.015803)
- Typep, S., Oertel, M., Klähn, T., et al. 2022, arXiv e-prints, arXiv:2203.03209. <https://arxiv.org/abs/2203.03209>
- van der Walt, S., Colbert, S. C., & Varoquaux, G. 2011, Comput. Sci. Eng., 13, 22, doi: [10.1109/MCSE.2011.37](https://doi.org/10.1109/MCSE.2011.37)
- Virtanen, P., et al. 2020, Nature Meth., doi: [10.1038/s41592-019-0686-2](https://doi.org/10.1038/s41592-019-0686-2)
- Wade, L., Creighton, J. D. E., Ochsner, E., et al. 2014, Phys. Rev. D, 89, 103012, doi: [10.1103/PhysRevD.89.103012](https://doi.org/10.1103/PhysRevD.89.103012)
- Walker, K., Smith, R., Thrane, E., & Reardon, D. J. 2024, arXiv e-prints, arXiv:2401.02604, doi: [10.48550/arXiv.2401.02604](https://doi.org/10.48550/arXiv.2401.02604)
- Wes McKinney. 2010, in Proceedings of the 9th Python in Science Conference, ed. Stéfan van der Walt & Jarrod Millman, 56 – 61, doi: [10.25080/Majora-92bf1922-00a](https://doi.org/10.25080/Majora-92bf1922-00a)
- Williams, N., Pratten, G., & Schmidt, P. 2022, Phys. Rev. D, 105, 123032, doi: [10.1103/PhysRevD.105.123032](https://doi.org/10.1103/PhysRevD.105.123032)
- Wiringa, R. B., Fiks, V., & Fabrocini, A. 1988, Phys. Rev. C, 38, 1010, doi: [10.1103/PhysRevC.38.1010](https://doi.org/10.1103/PhysRevC.38.1010)
- Woosley, S., Sukhbold, T., & Janka, H. T. 2020, Astrophys. J., 896, 56, doi: [10.3847/1538-4357/ab8cc1](https://doi.org/10.3847/1538-4357/ab8cc1)
- Wysocki, D., O'Shaughnessy, R., Wade, L., & Lange, J. 2020, arXiv e-prints, arXiv:2001.01747, doi: [10.48550/arXiv.2001.01747](https://doi.org/10.48550/arXiv.2001.01747)